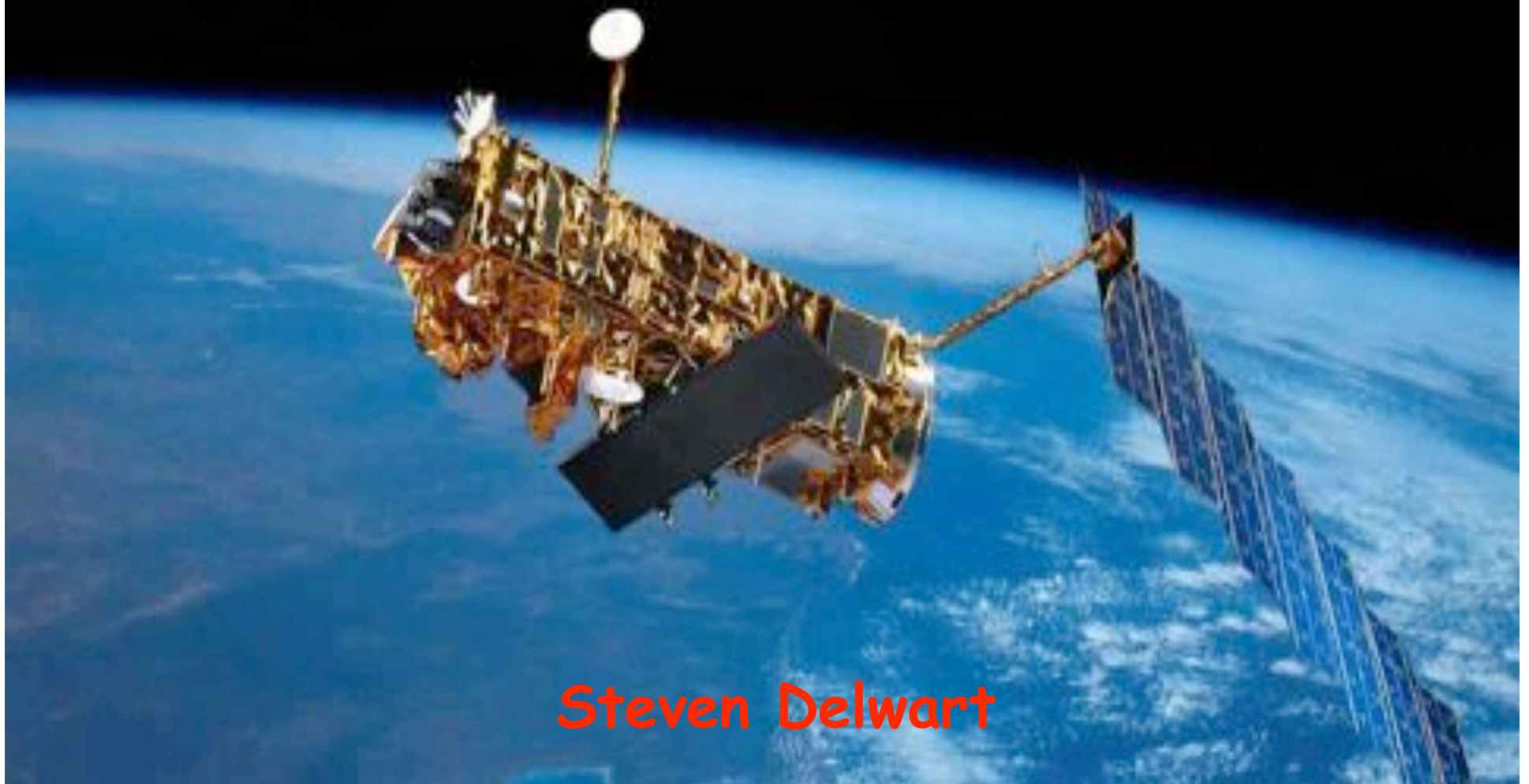


MERIS US Workshop

Vicarious Calibration Methods and Results



Steven Delwart

Recent results

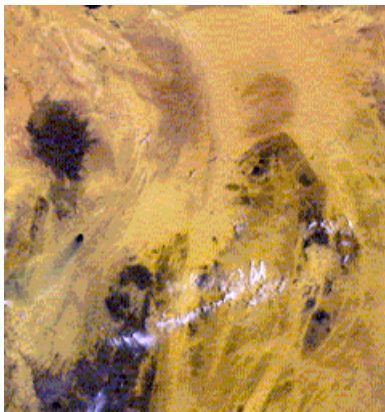
1. CNES methods
Deserts, Sun Glint, Rayleigh Scattering
2. Inter-sensor Uyuni
3. MOBY-AAOT
4. Vicarious Adjustment methodology

Older results

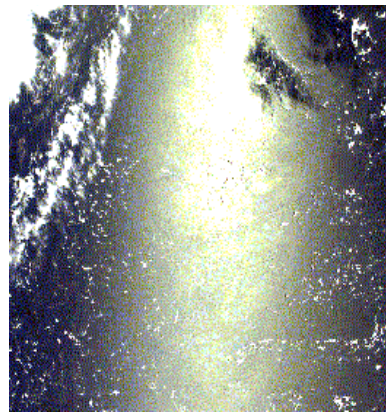
1. Dark Water
2. SIMBADA Ocean
3. Rail Road Valley Playa
4. Comparison with AATSR
5. Comparison with SCIAMACHY
6. Snow Targets

Calibration of MERIS using natural targets

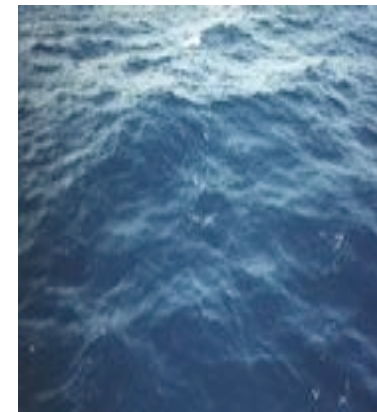
Deserts, Sun Glint, Rayleigh Scattering
(Claire Tinel, Patrice Henry, Olivier Hagolle - CNES)



Deserts



Sun glint



Rayleigh

These calibration methods are used operationally at CNES
for POLDER 1, 2, 3, VEGETATION 1 and 2,
for SPOT satellites, MERIS, FORMOSAT-2 and KOMPSAT-2

Calibration of MERIS using natural targets

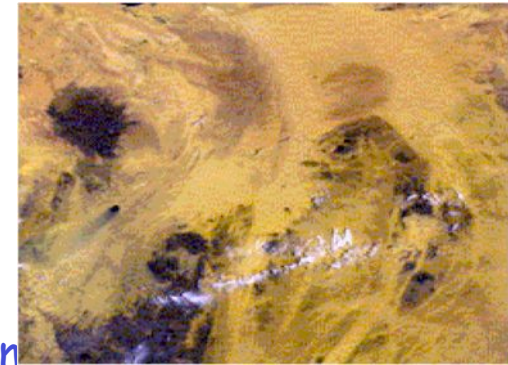
- Definitions
 - Meris on board calibration is the nominal calibration method
 - Meris is calibrated against t.o.a. reflectance

$$DN_k = A_k \cdot \tilde{n}_k \cdot \cos(\epsilon_s)$$

- k: Spectral band
- DN : Digital Number (Meris Level 0, corrected for instrumental defects)
- r : Reflectance
- A : Sensitivity of instrument for spectral band k

$$\ddot{A}A_k = \frac{A_{k,method}}{A_{k,L1}} = \frac{\tilde{n}_{k,measured(L1)}}{\tilde{n}_{k,predicted} (Method)}$$

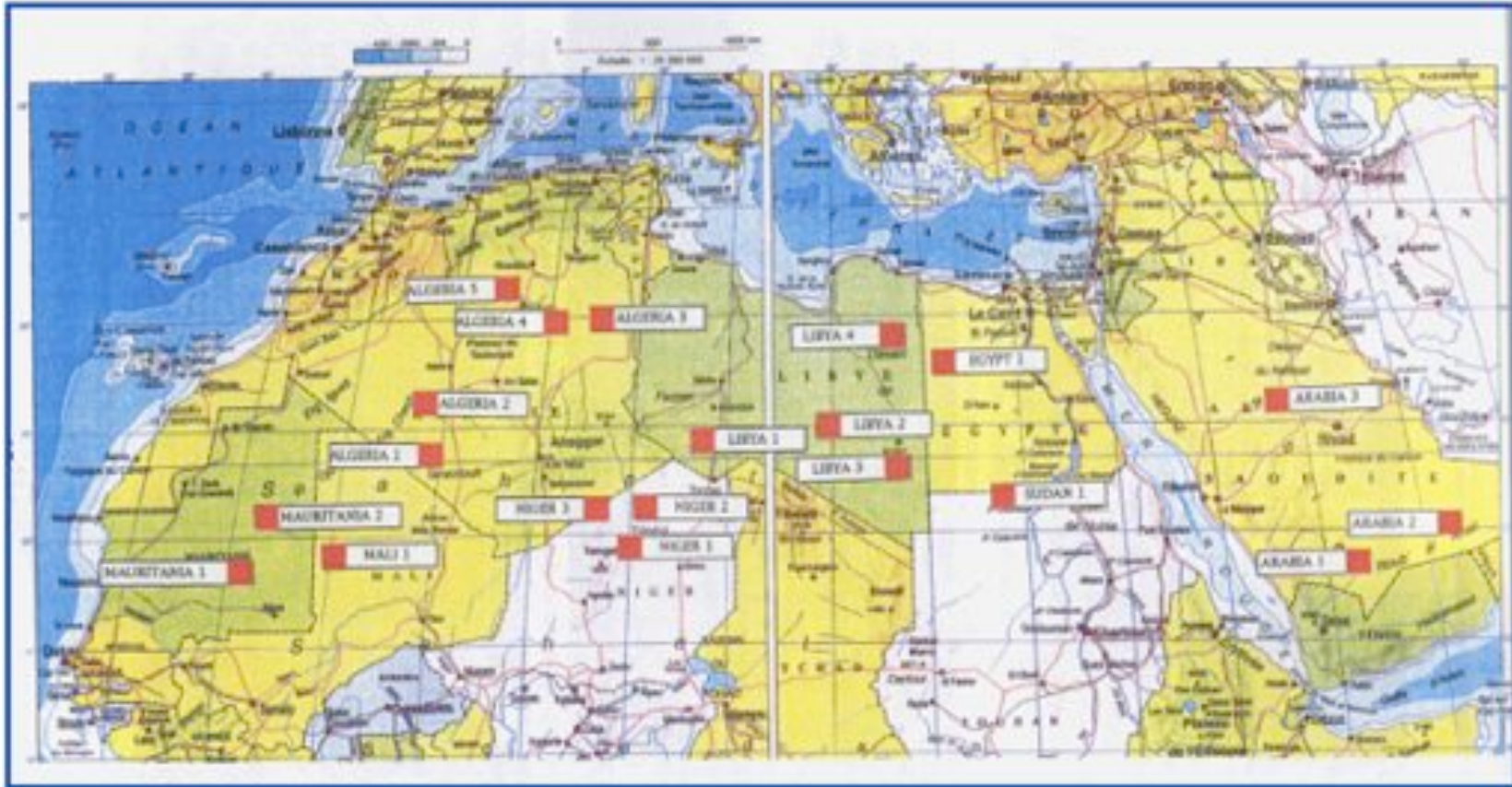
- Initial objectives :
 - In orbit vicarious calibration to assess :
 - Multiangular calibration (detectors normalization in the f.o.v.)
 - In time calibration monitoring (on-board calibration verification)
 - Intercalibration of sensors



- Main characteristics of the requested sites :
 - Stable in time : no vegetation...
 - Easy to access : low cloud coverage, good atmospheric conditions
 - High reflectance : to reduce the impact of atmospheric effects
 - Low directional effects

⇒ **Choice : Desert sites**

- Sites selection :



- Systematic collect of satellite acquisition
Operational monitoring of CNES sensors

- SPOT(s)/High Resolution
- SPOT(s)/Vegetation-1&2
- PARASOL

Calibration monitoring and intercalibration
(through cooperation agreements with CNES)

- High resolution : Formosat-2 (Taiwan)
- Medium resolution : MERIS (ESA), MODIS (NASA)

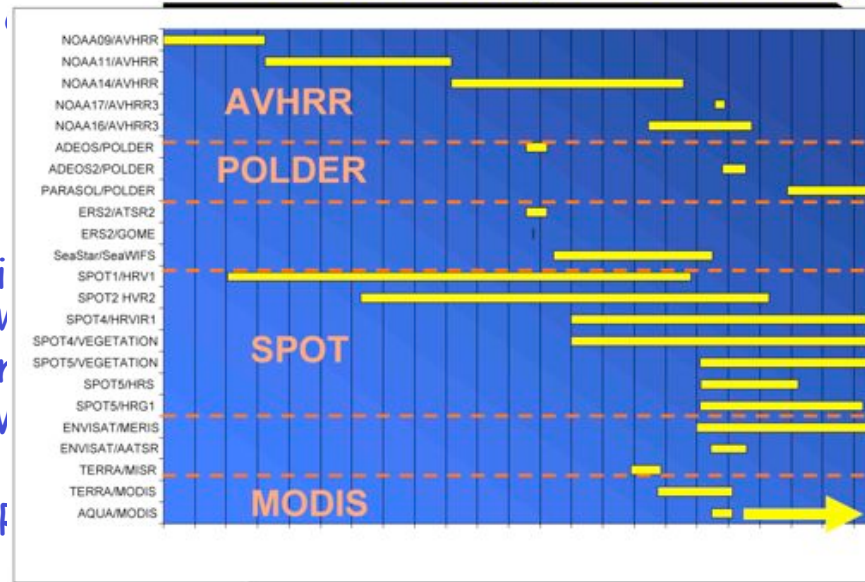
Archive of POLDER1&2, SeaWiFS, AVHRR

- Storage in a data base :

- SADE data base : "Structure d'Accueil de Données d'Etalonnage"
(*Calibration Data Repository*)
- Easy data management
- Link between satellite measurements and calibration results (traceability)

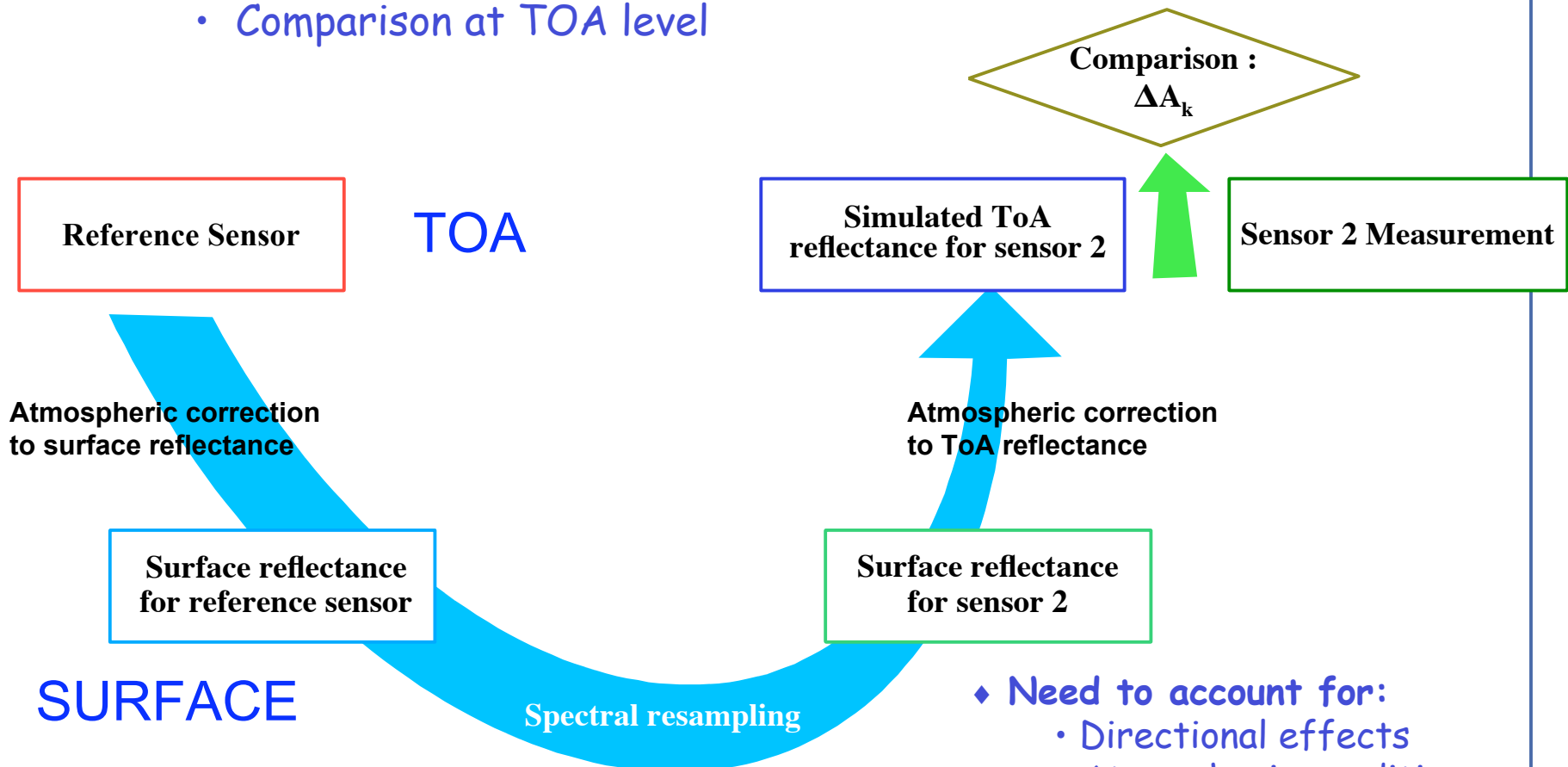
- Nota : the SADE data base also includes calibration measurements over ocean, sun glint, clouds and snow covered sites.

Desert Sites Database (from 1985 until 2007)



Method

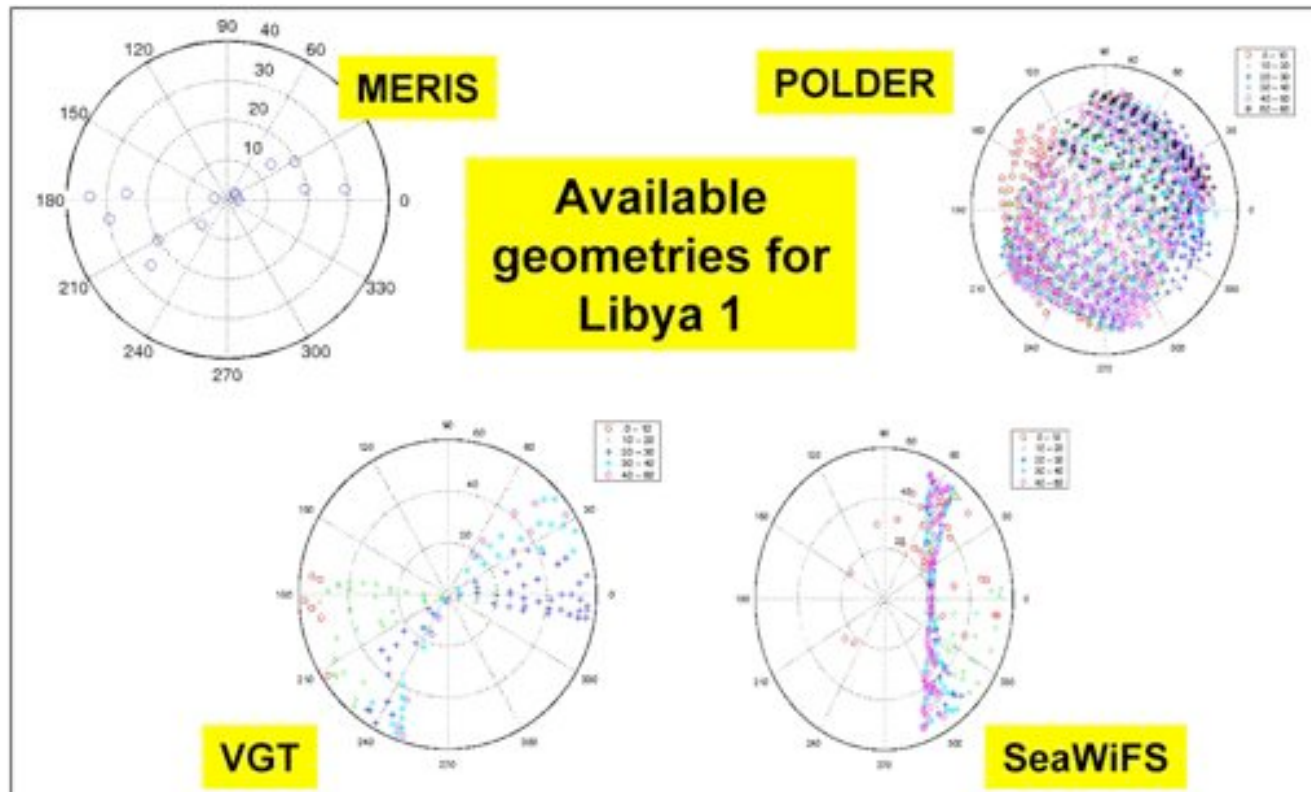
- Compare two sensors :
 - One sensor as reference
 - Comparison at TOA level



- ♦ Need to account for:
 - Directional effects
 - Atmospheric conditions
 - Spectral discrepancies

Geometry

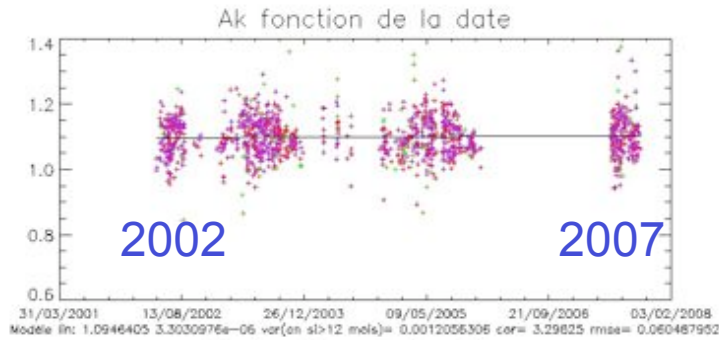
- Directional effects :
 - Direct comparison of measurements in the same geometry (qs , qv , f)
 - Use of reciprocity principle to extend field of matching geometries



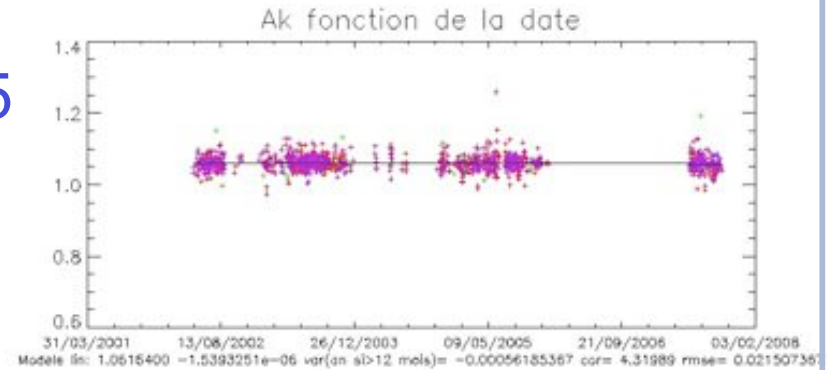
Processing

- Atmospheric correction :
 - Atmospheric correction performed using SMAC and meteo data :
 - Rayleigh scattering correction
 - Water vapour
 - Ozone
 - Other contributors : CO₂, CO, NO₂, CH₄ (climatologies)
 - Problem : aerosol correction...
 - Aerosol optical thickness $\tau = 0.2$
 - Statistically solved through the use of a lot of data:
no significant bias, but dispersion for short wavelengths

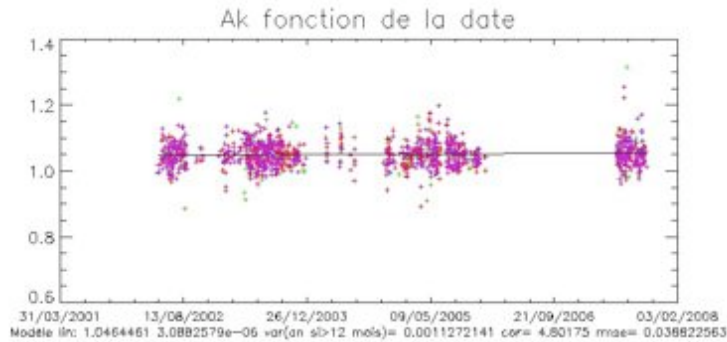
490



865

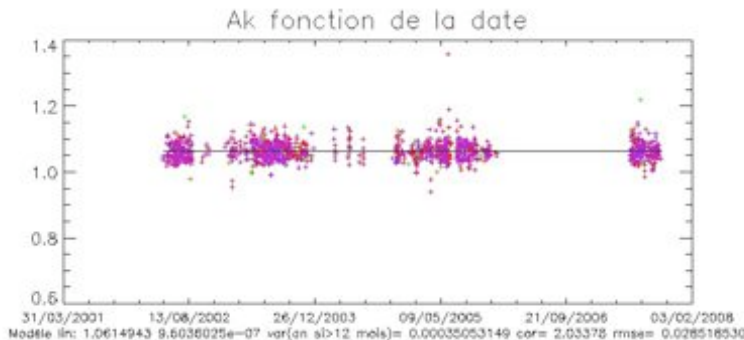


560



Cross-calibration with PARASOL as a function of time (20 sites)

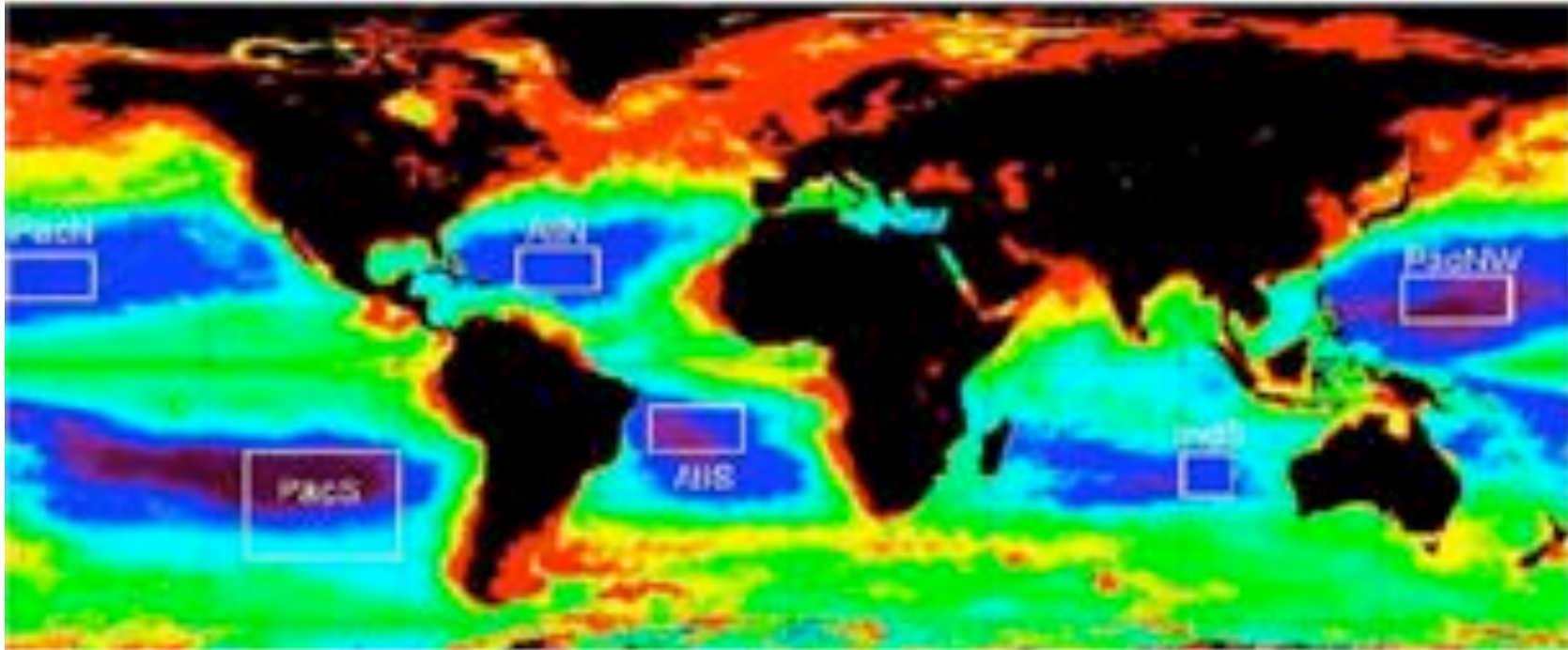
665



No significant variation with time

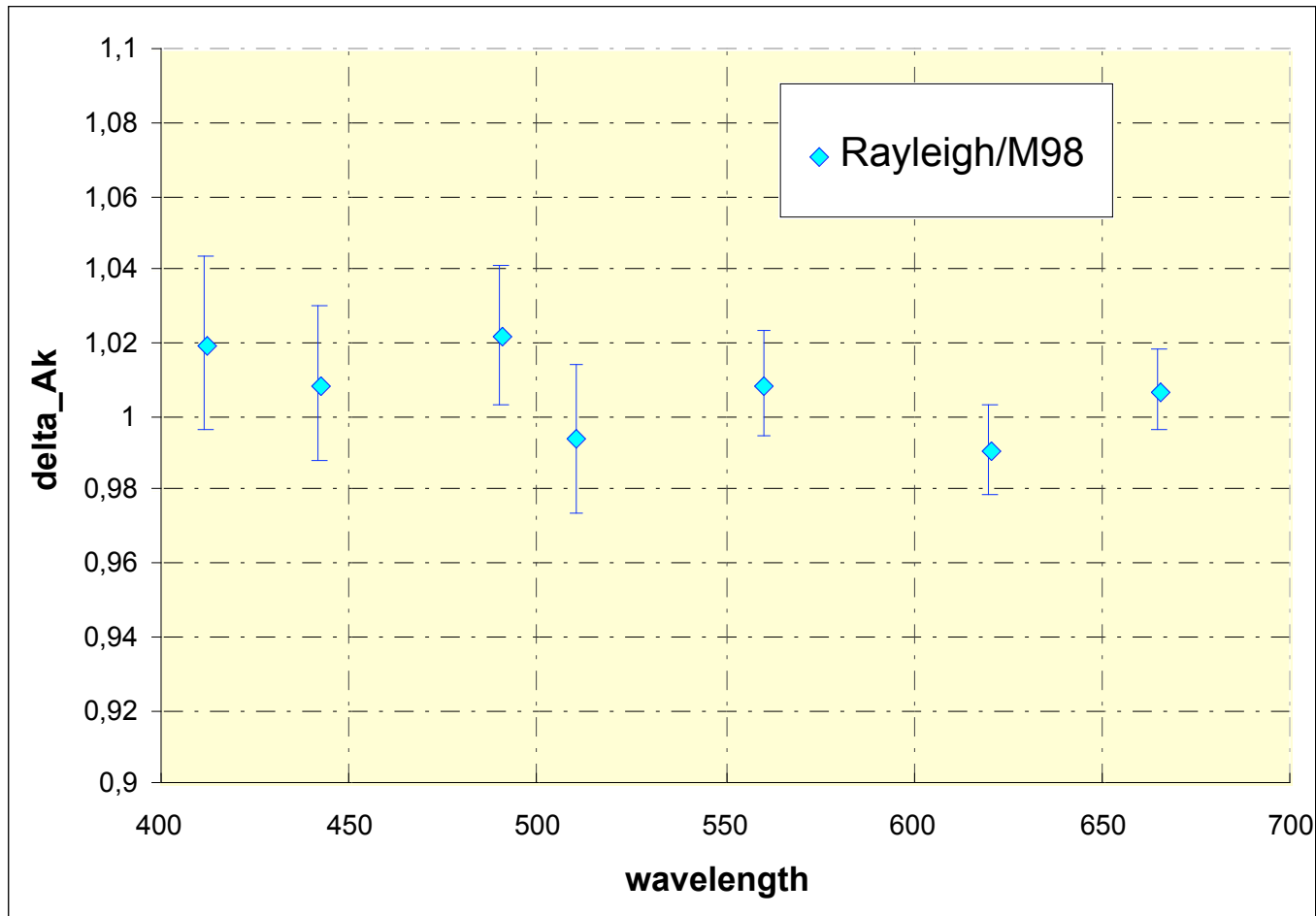
- Observe the atmosphere over ocean (dark)
- Absolute calibration of bands < 700 nm
- Rayleigh scattering : $> 80\%$ of signal
- TOA reflectance well predicted using:
 - Successive Orders of Scattering
 - Smile effect correction
- Main error sources
 - ocean surface reflectance :
 - predicted using climatology derived from SeaWiF
 - only over very stable oceanic zones (oligotrophic zones)
 - aerosols : estimated using 865 nm band
 - Only optical thickness < 0.1 are kept
- Accuracy : 4 to 5% (3s) - 2 to 3 % (RMS)





Choice of oligotrophic areas with 2 years of SeaWiFS data made in 2001 with ACRI and LOV (CLIMZOO zones)

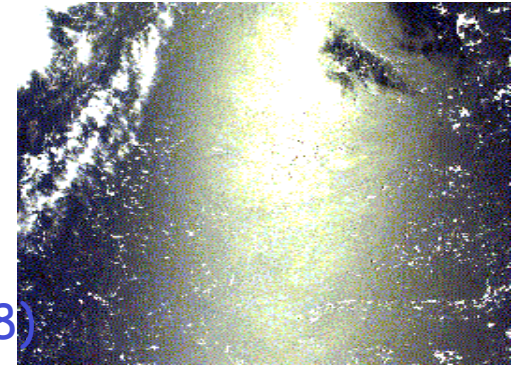
Results



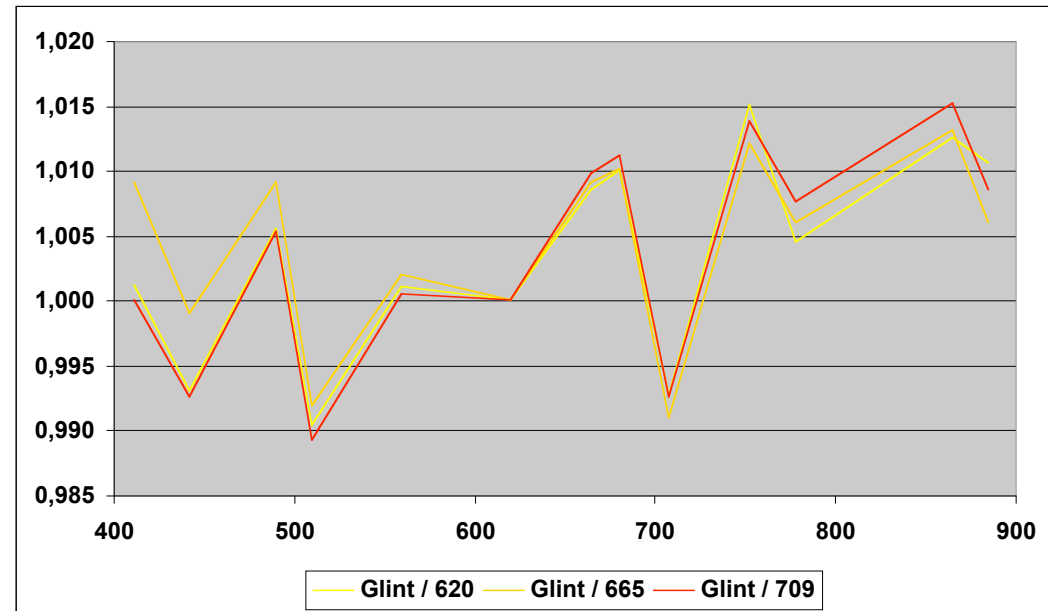
No discrepancy greater than 2.5%

Calibration of MERIS using natural targets

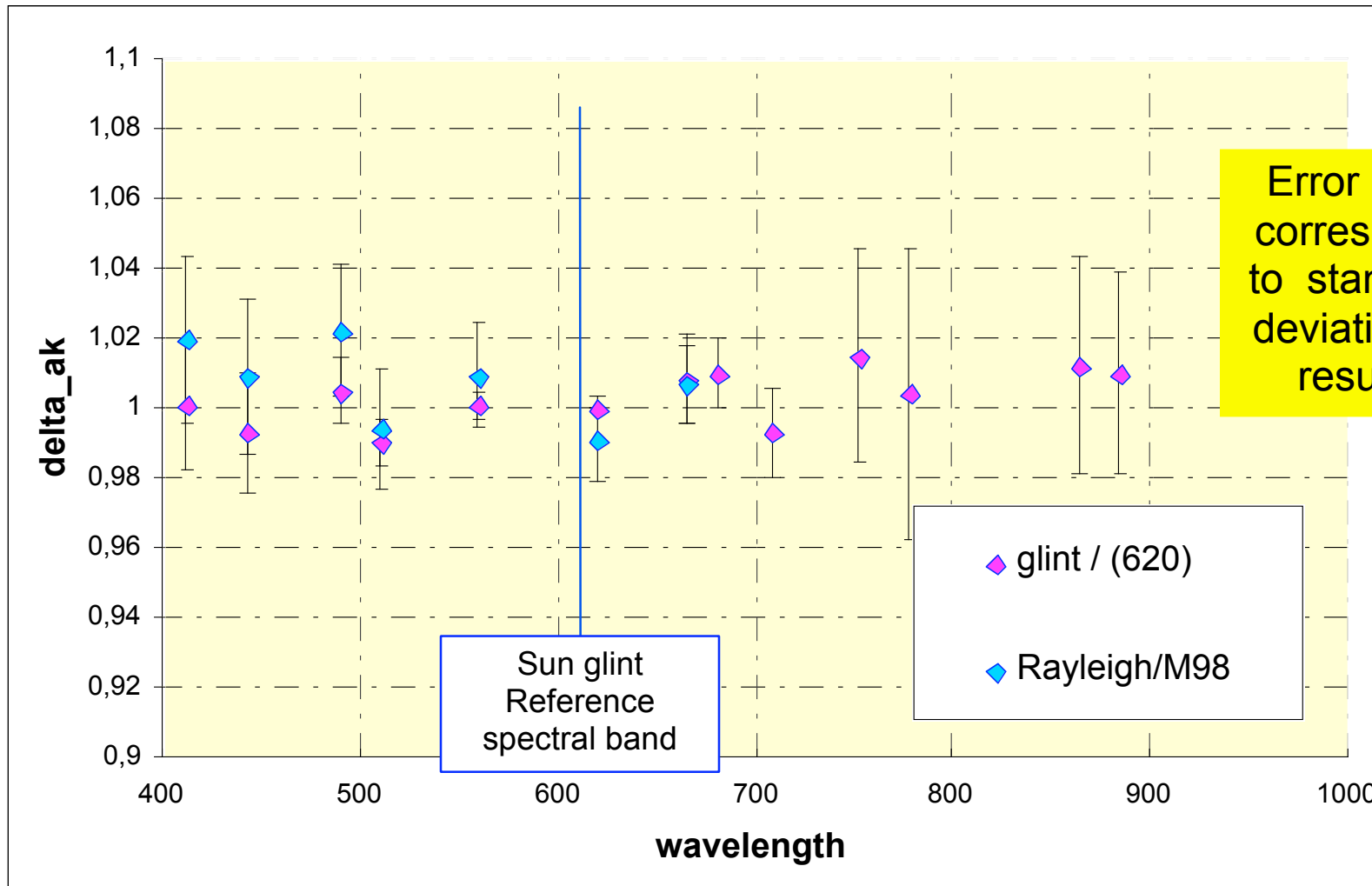
- Sun glint calibration
 - observe the white reflection of the sun over the ocean surface
 - interband calibration w.r.t. a reference spectral band
 - TOA reflectance predicted using SOS code
- Main error sources
 - Reference band calibration errors
 - ocean surface : SeaWiFS climatology
 - aerosols : fixed model used (M98, AOT :0.08)
 - daily SeaWiFS aerosol product used to discard cases when aerosol properties differ from reference model
- Accuracy : 3 to 4.5% (3s) - 1.5 to 2% (RMS)



Band	Ref Band 620		Ref Band 708	
	ΔA_k	σ	ΔA_k	σ
412	1.001	0.019	1.007	0.022
442	0.993	0.017	1.000	0.020
490	1.005	0.010	1.013	0.016
510	0.990	0.007	0.997	0.130
560	1.001	0.004	1.008	0.013
620	-	-	1.007	0.011
665	1.008	0.013	1.017	0.008
681	1.010	0.010	1.019	0.008
708	0.993	0.013	-	-
753	1.015	0.031	1.021	0.026
778	1.004	0.042	1.015	0.021
865	1.012	0.031	1.023	0.016
885	1.010	0.029	1.016	0.024



Comparison of sun glint results using different reference bands



Still no discrepancy greater than 2.5%

Calibration of MERIS using natural targets

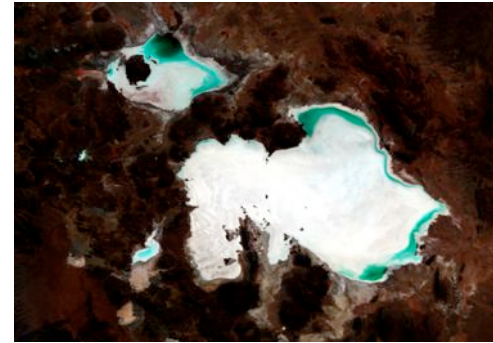
- Conclusions
 - MERIS instrument seems well calibrated
 - Rayleigh + glint + deserts
 - measurements agree with MERIS level 1 calibration (within 2 %)
 - Very good agreement between Rayleigh and sun glint calibration methods
 - no significant degradation with time
 - thanks to :
 - » MERIS calibration device
 - » MERIS good spectral calibration
 - Simultaneous validation of :
 - MERIS calibration
 - CNES calibration methods
- Perspective
 - Multitemporal calibration monitoring of 412 and 443 nm bands
 - MERIS/MODIS intercalibration over deserts

Data Selection Criteria: Reciprocal and identical doublets are kept if from the same day or differing by one day

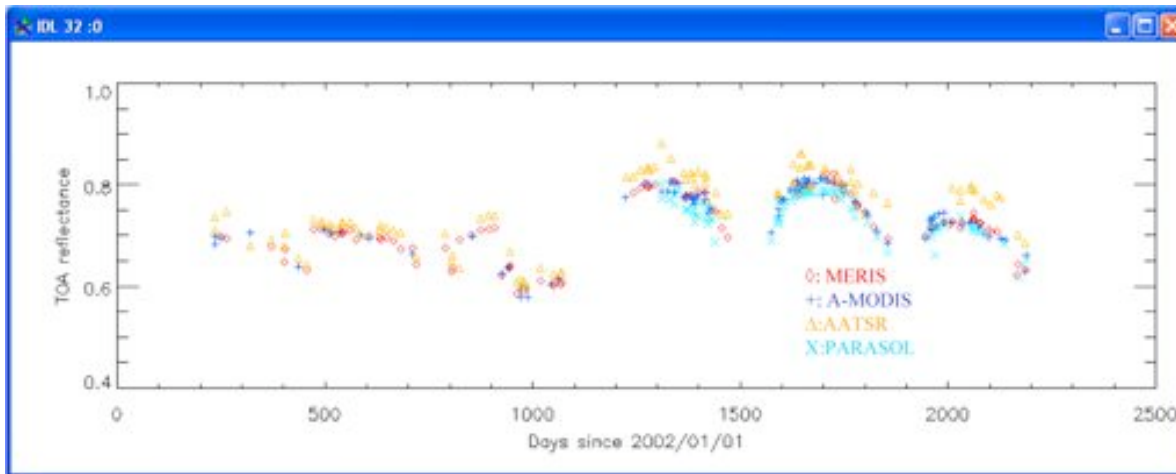
Geometric selection criteria

$$10 \text{ deg} > \sqrt{[(\text{SZA}(i) - \text{SZA}(j))^2 + (\text{VZA}(i) - \text{VZA}(j))^2 + 1/4 \times (\text{abs}(\text{RAA}(i)) - \text{abs}(\text{RAA}(j)))^2]}$$

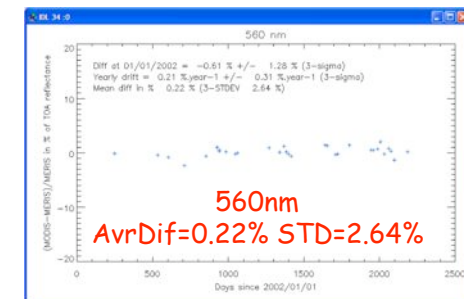
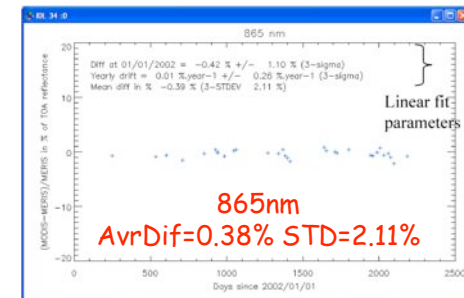
(Equivalent to a difference of 5 deg for VZA & SZA and ± 10 for RAA.)



Salar de Uyuni (Bolivia)



Sensor Intercomparison
MERIS, MODIS, AATSR, PARASOL

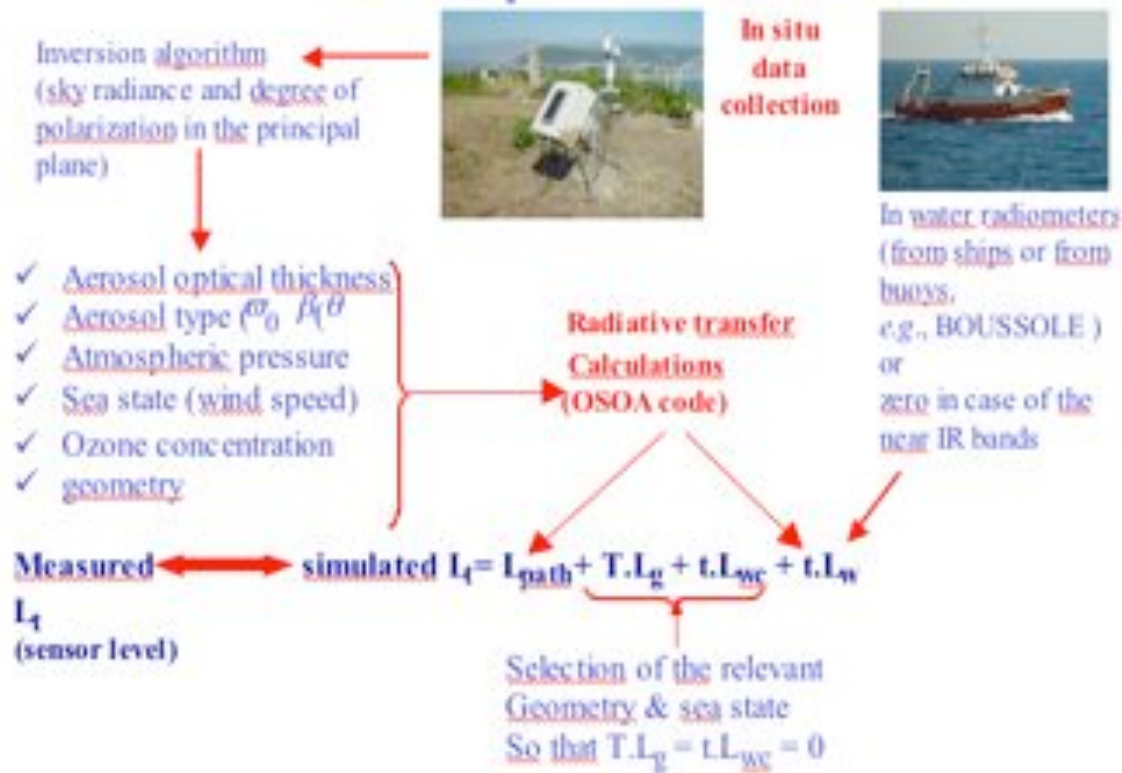


MODIS vs MERIS
Very good agreement

LISE Analysis Moby, AAOT

MERIS vicarious radiometric calibration

Reconstruction of the Top-of-the-atmosphere (TOA) total radiance, to be compared to its observed value



Careful selection of input data ==> uncertainty budget <5% in the near infrared & ~3% in the visible

Aerosol	[nm]	412	443	490	520
Venise AAOT					
IOPA	Slope	0.972	0.970	0.953	0.965
	R ²	0.98	0.97	0.93	0.92
Junge	Slope	1.019	1.018	1.004	1.016
	R ²	0.80	0.90	0.86	0.85
SAM	Slope	0.996	0.994	0.979	0.991
	R ²	0.90	0.90	0.84	0.83
MOBY					
IOPA	Slope	0.957	0.951	0.927	0.910
	R ²	0.87	0.79	0.56	0.27
Junge	Slope	0.972	0.967	0.946	0.930
	R ²	0.84	0.76	0.51	0.21
SAM	Slope	0.961	0.954	0.930	0.912
	R ²	0.83	0.74	0.48	0.16

Good agreement in the blue, questionable in the NIR do to dominant backscattering geometry available from Moby.

Aerosol	[nm]	753	778	865
Venise AAOT				
IOPA	Slope	0.870	0.880	0.876
	R ²	0.89	0.88	0.86
Junge	Slope	0.910	0.900	0.879
	R ²	0.86	0.87	0.87
SAM	Slope	0.865	0.852	0.825
	R ²	0.81	0.80	0.80
MOBY				
IOPA	Slope	0.660	0.635	0.566
	R ²	-2.51	-2.46	-2.00
Junge	Slope	0.681	0.654	0.570
	R ²	-2.00	-1.99	-1.75
SAM	Slope	0.961	0.954	0.930
	R ²	-3.11	-3.21	-3.08

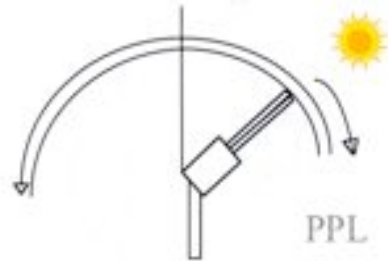
Older results

- Dark Water
- SIMBADA Ocean
- Rail Road Valley Playa
- Comparison with AATSR
- Comparison with SCIAMACHY
- Snow Targets

METHODOLOGY

-We use PPL radiance measurements instead of only AOT

-Method reported in *Santer & Martiny* (AO, fev2003) :
Computation of phase function as follows:



1- Correction of PPL measurements using the f corrective factor (correction for multiple scattering effects) :

$$f = \left(\frac{L(1)}{L} \right)_{theo} \approx \left(\frac{L(1)}{L} \right)_{mes}$$

- Order 0, f simulated with Junge Power Law as input of RTC (SOS)

- Iterations stop when f converges at 0.5%

2- Approximation of primary scattering :

(SOS) f at order $n+2$

$$P(\Theta) = 4L_{scat}^{(1)} \exp\left(\frac{\tau}{\mu}\right) \left[1 - \exp\left(-\tau\left(\frac{1}{\mu_0} - \frac{1}{\mu}\right)\right) \right]^{-1} \left[\frac{\mu_0}{\mu - \mu_0} \right]^{-1}$$

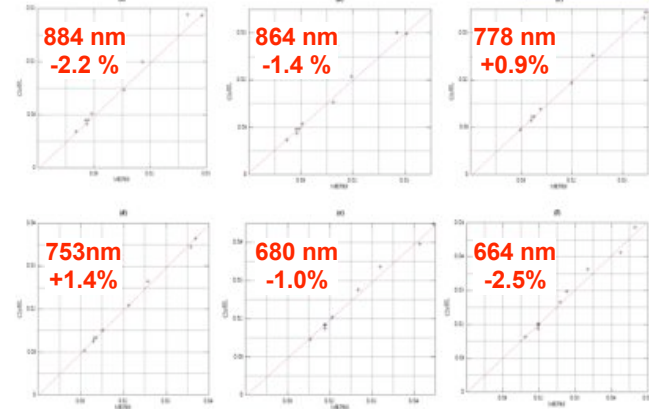
Total Phase Function *
Total Single scattering albedo

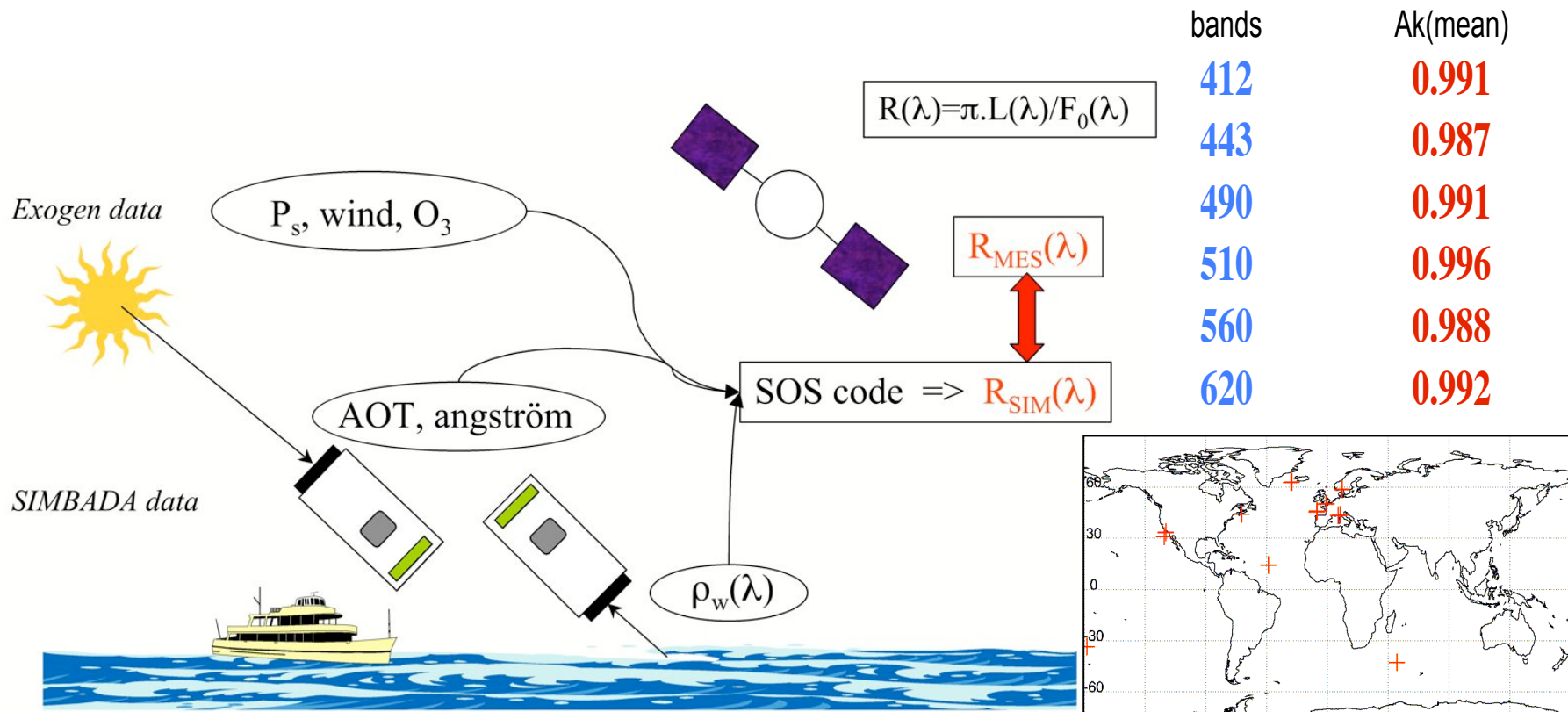


Simulated MERIS Radiances

RESULTS from 884 to 664 nm

2 sites, 9 days
Cakoff (2) / Venice (7)



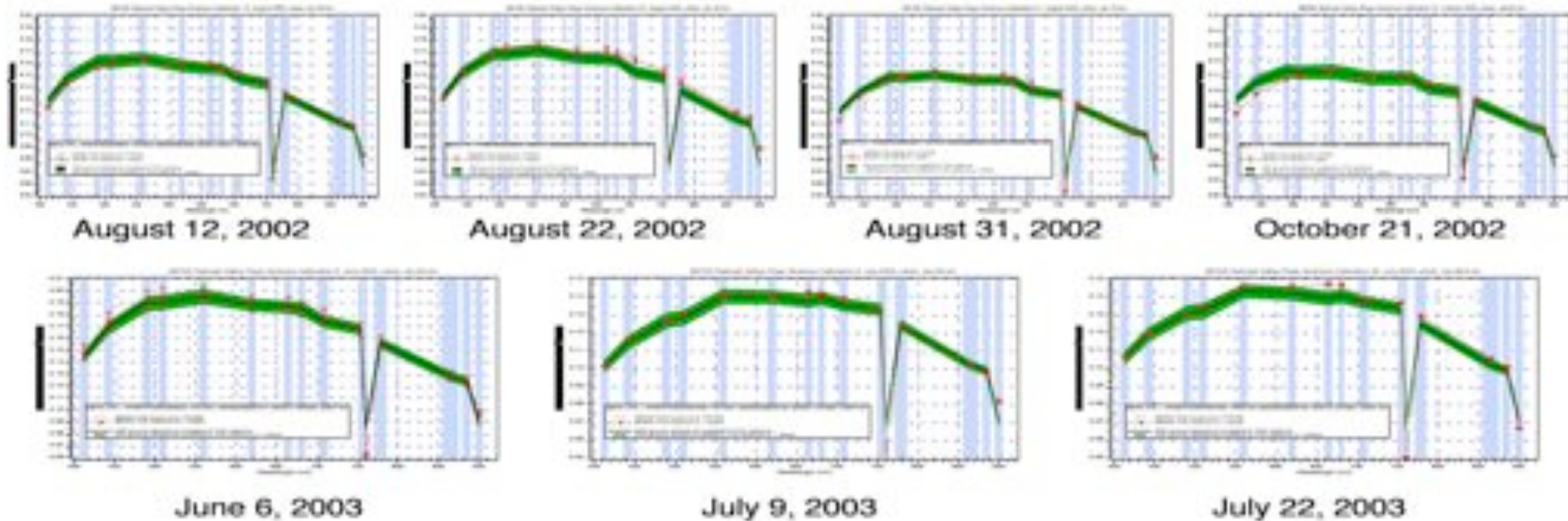


- Successive Order of Scattering (SOS) code from LOA/CNES
- Threshold :
 - AOT(865 nm) < 0.15
 - Measurement within +/- 3 hours from satellite overpass
 - No case 2 waters (high reflectance at 560 nm)

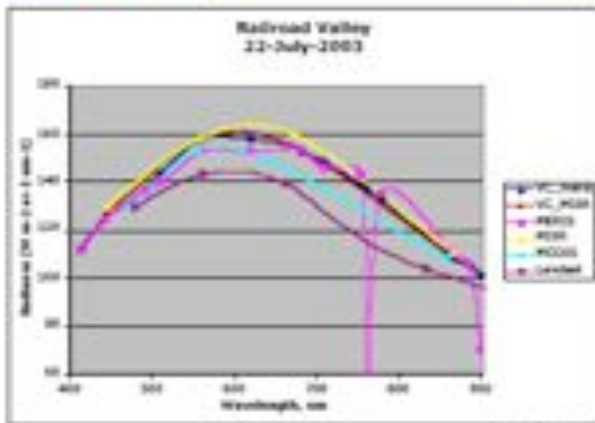
- 23 independant pixels from 14 scenes
- AOT max : 0.15
- Within 3 hours from satellite overpass
- Case 2 waters rejected

Collaboration RSL & UofA

MERIS	Center	(%)	(%)	(%)	(%)	(%)	(%)	(%)
1	412.545	-4.481	-0.604	-6.614	-10.879	3.080	-0.330	0.565
2	442.401	-5.193	-0.844	-3.141	-7.658	2.825	0.782	0.138
3	489.744	-4.861	-0.335	-1.267	-5.069	1.024	-0.541	-0.221
4	509.700	-2.037	2.356	1.147	-1.624	2.221	1.161	1.834
5	559.634	-1.727	2.543	1.530	0.054	0.832	0.449	2.080
6	616.620	-0.881	3.035	1.325	0.634	0.471	0.353	2.491
7	664.640	0.398	4.028	1.805	1.317	0.912	3.252	5.444
8	680.902	-0.123	3.442	0.674	0.298	-0.020	1.337	3.984
9	708.426	2.480	5.884	3.657	3.282	2.287	2.486	1.460
10	753.472	0.573	3.856	0.218	0.097	-0.387	-0.955	2.238
12	778.498	1.820	5.011	0.941	1.195	0.492	-0.097	3.388
13	864.833	1.622	4.512	-0.026	0.550	0.321	-0.364	3.096
14	884.849	1.619	4.465	-0.436	-0.083	-0.324	-0.950	2.253
Mean diff (%)	All Bands	1.820	2.140	1.752	2.518	1.169	1.004	2.246

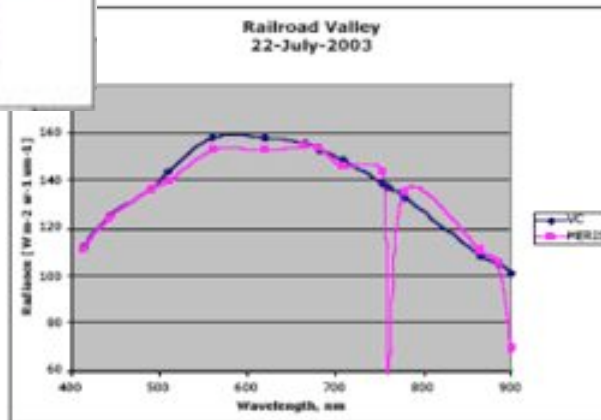


Collaboration JPL & UofA



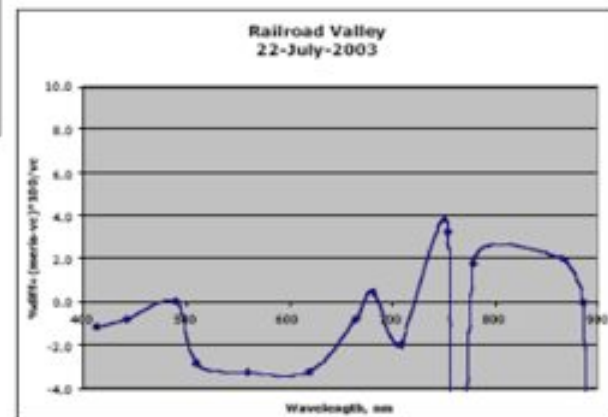
MISR/ MERIS measured radiances agree to within +/- 3%

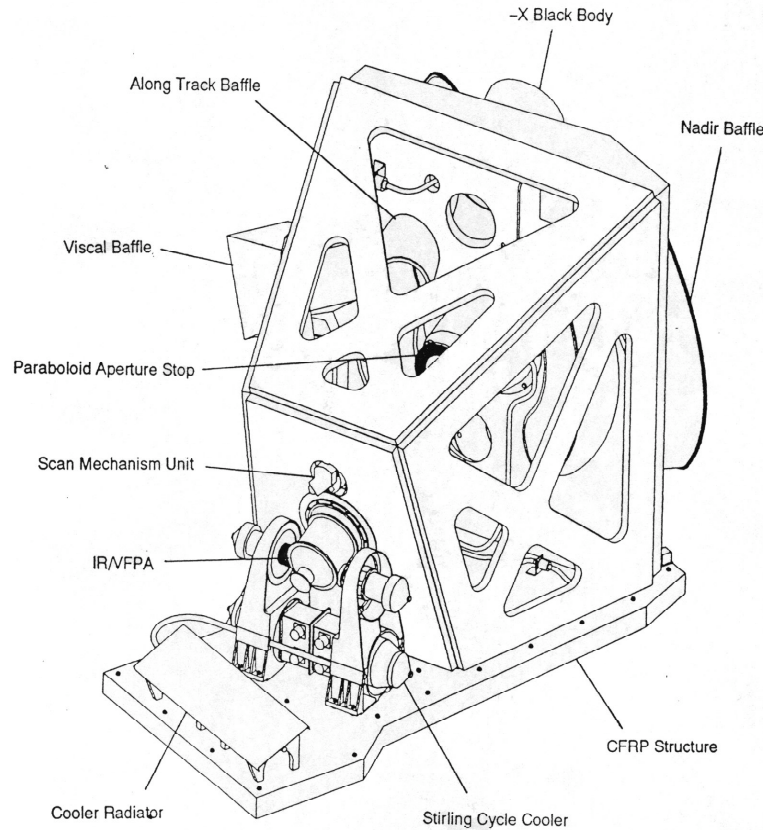
MERIS data confirm that VC scale is consistent, band-to-band, with AirMISR, MODIS band-relative scale



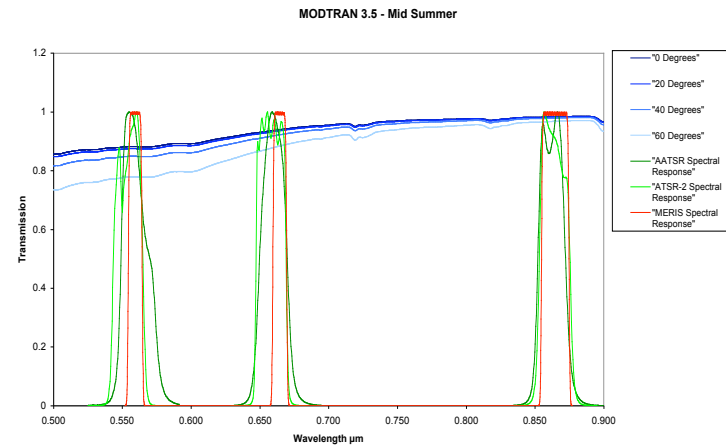
MERIS radiances include 1.04 adjustment due to Terra/ Envisat time difference.

Agreement with VC computed radiances is generally within 4%.

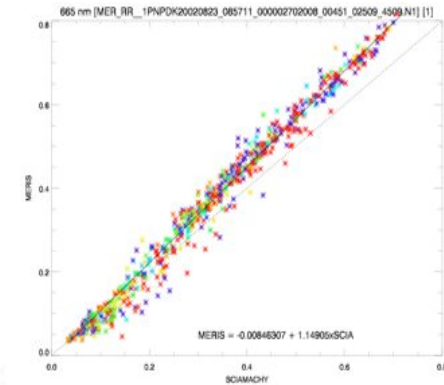
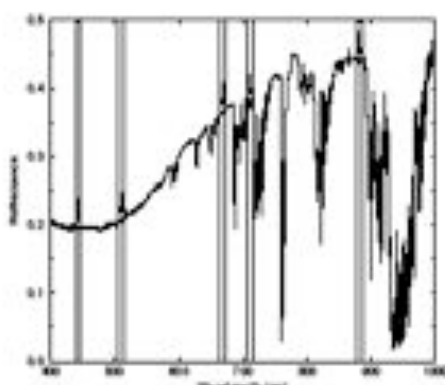
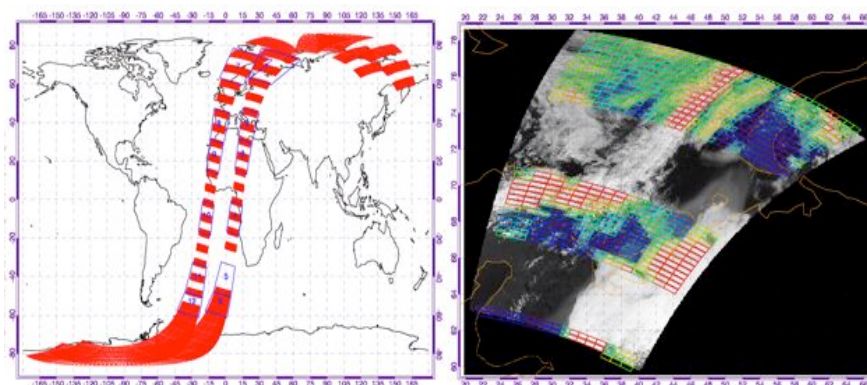




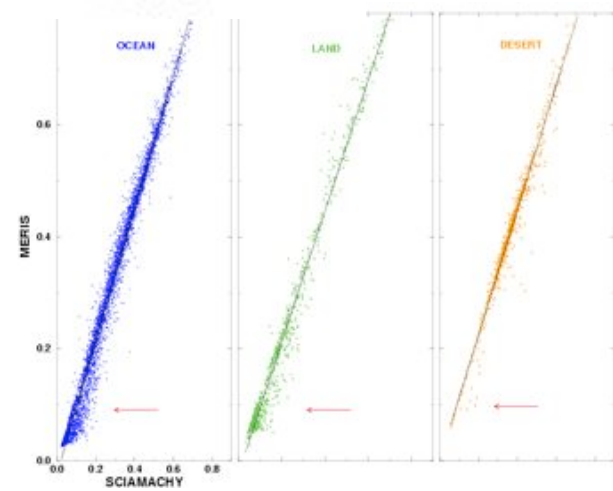
Surface	560 nm	670 nm	870 nm
Deserts (Smith)	1.041	1.001	1.037
Greenland (Smith)	1.034	1.012	1.037
Clouds (Poulsen)	1.047	1.026	1.054
Longyeardyen	1.026	1.024	1.038
Barrows	1.024	1.001	1.023



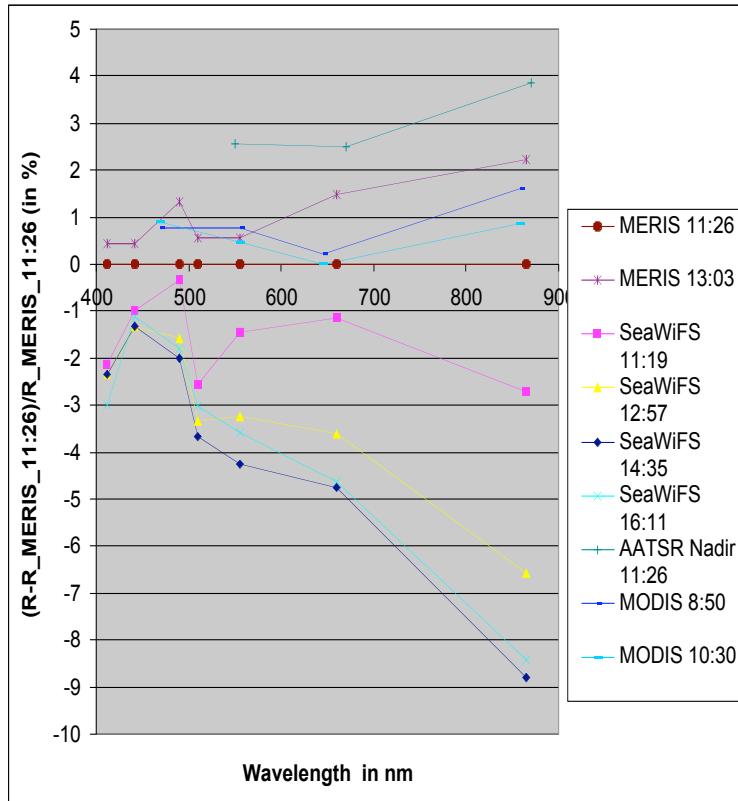
esa Comparison with SCIAMACHY



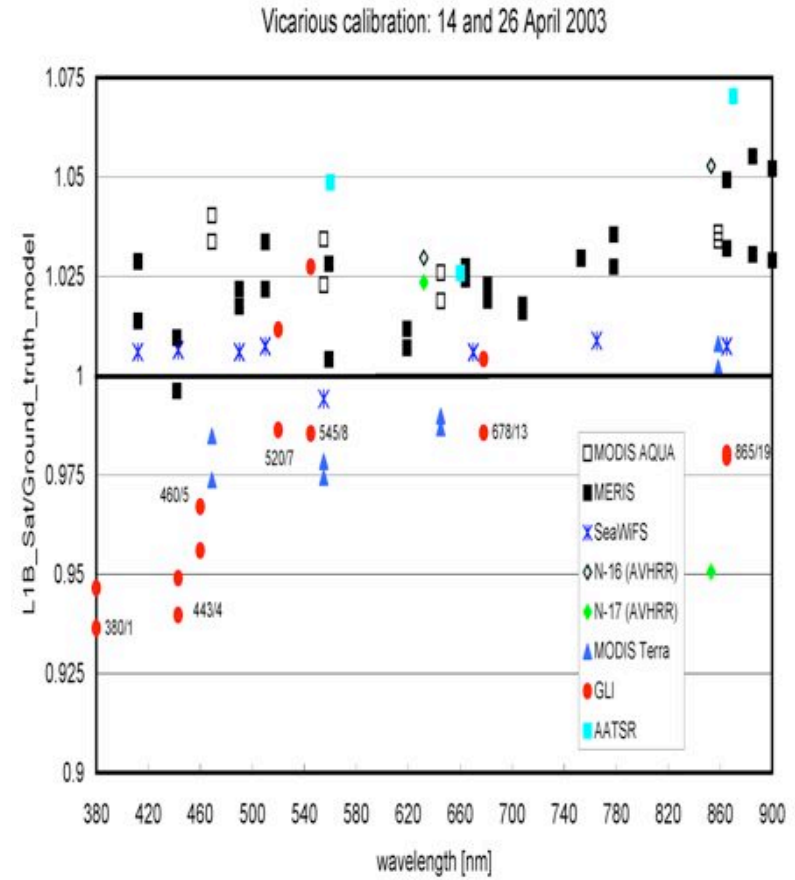
Slope	1.18	1.17	1.19	1.21	1.25
	1.15	1.16	1.17	1.19	1.20
	1.10	1.09	1.12	1.12	1.15
Offset	-0.026	-0.023	-0.024	-0.023	-0.027
	-0.022	-0.022	-0.023	-0.020	-0.012
	-0.004	0.000	0.002	0.010	0.013
Corr.	0.993	0.992	0.990	0.989	0.988
	0.990	0.988	0.990	0.988	0.987
	0.988	0.985	0.985	0.980	0.976



- Given the current state of knowledge, we (KNMI) propose that it is the reflectance data of SCIAMACHY instead of MERIS, that should be corrected.



Longyearbyne (ESA)



Barrows (JAXA)

Vicarious Adjustment Principle

- Based on the work currently lead at NASA for SeaWiFS and MODIS vicarious calibration, see Franz et al. 2007, Bailey et al. 2007.
- Consists in computing averaged multiplicative gains to correct the "TOA signal", thanks to a DB of reference in-situ signals:
 - « TOA signal » = Level 2 reflectance pre-corrected for smile, gaseous absorption, glint, *i.e.* just before the Atmospheric Correction algorithm.
 - $\rho_{gc}^{new}(l) = \rho_{gc}(l) * G(l)$ for l in the VIS and NIR
- Two-step approach separating the NIR and VIS channels, avoiding an iterative procedure within the Atmospheric Correction algorithm:
 1. First adjust two bands in the NIR with $G(l_{NIR})$
 2. Then, assuming a perfect AC, adjust the VIS with $G(l_{VIS})$
- The methodology fully imbricates the sensor response and the processing:
 - The gains need to be updated each time a change occurs in the processing (LUTs, algorithm, Lib calibration, etc.)
 - a strong effort of traceability in the gain computation, with respect to all other processing parameters, should be maintained.

- Computation starts from the decomposition

$$r_{gc}(l) = r_{path}(l) + t_d(l)r_w(l)$$

- Knowing the true (or targetted) signal through in-situ measurements, individual gains are computed matchups per matchups by

$$g_i(l) = [r_{path}^t(l) + t_d^t(l)r_w^t(l)] / [r_{path}(l) + t_d(l)r_w(l)]$$

- Averaged gains are finally deduced by $G(l) = \text{Mean } g_i(l)$

- In the NIR, two assumptions:

- the water-leaving reflectance is truly negligible: $r_w(l_{NIR}) = 0$
- the most NIR band (865 nm for MERIS) is perfectly calibrated : $g_i(865) = 1$

- Thus one has

$$r_{gc}^t(865) = r_{gc}(865) = r_{path}(865)$$

$$r_{gc}^t(775) = g(775) * r_{gc}(775) = r_{path}^t(775).$$

- DB : oligotrophic sites ($\rightarrow r_w = 0$) + homogeneity in space and time (\rightarrow alpha)

- In the VIS, once the NIR is calibrated, gains are computed thanks to

$$r_{path}^t(l_{VIS}) = r_{path}(l_{VIS}) \quad \text{and} \quad t_d^t(l_{VIS}) = t_d(l_{VIS})$$

$$r_w^t(l_{VIS}) = r_w^{in-situ}(l_{VIS})$$